SIMULATION AND EXPERIMENTAL RESEARCH OF DRIVER SYSTEM AND STARTING PROCESS OF A CONE INERTIAL CRUSHER

Petko Nedyalkov[1], Simeon Savov[2]

[1] *Technical University of Sofia, 1756 Sofia, e-mail: nedpetko@tu-sofia.bg*
[2] *University of Mining and Geology "St. Ivan Rilski", 1700 Sofia, e-mail: ss.ss@abv.bg*

ABSTRACT. The presented methodic follows the steps of installed machine power dynamical research in order to find the more economical way of materials crushing and effective power usage. The paper deals with the study of the starting process of the unbalanced vibrator within comparison between theoretical simulation model and experimental results. There are presented dynamical simulation model with applied speed–torque characteristics of induction motor and some results with different machine settings. The simulation results are compared with experimental recordings from a real machine experiment. The dynamical model is using a Mat Lab simulation of differential equations system with application of non linear driver and resistance torque representing the real cone inertial crusher type KID-300 construction and physical parameters.

Key words: dynamical model, speed up process, torque, power, cone inertial crusher, unbalanced vibrator, speed torque induction motor characteristic

СИМУЛАЦИОННО И ЕКСПЕРИМЕНТАЛНО ИЗСЛЕДВАНЕ НА ЗАДВИЖВАНЕТО И ПУСКОВИЯ ПРОЦЕС НА КОНУСНА ИНЕРЦИОННА ТРОШАЧКА
Петко Недялков[1], Симеон Савов[2]
[1] *Технически университет – София, 1756 София, E-mail: nedpetko@tu-sofia.bg*
[2] *Минно-геоложки университет „Св. Иван Рилски", 1700 София, E-mail: ss.ss@abv.bg*

РЕЗЮМЕ. Представената методика е построена по стъпките на динамично изследване на инсталираната мощност, търсейки по-ефективни начини за трошене на материалите и подобряване на ефективността на използване на енергията. В статията е описано изследване на пусковия процес на дебалансен центробежен вибратор и сравнение между теоретичен симулационен модел и експериментални резултати. Представен е динамичен модел с използване на механичната характеристика на задвижващия асинхронен двигател при някои особени настройки на машината. Симулационните резултати са сравнени със записи от натурен експеримент. Динамичният модел използва Mat Lab симулация на съставената система диференциални уравнения с нелинейна дясна част, описваща поведението на конусна инерционна трошачка тип КИД-300 с нейните конструктивни и физически показатели.

Ключови думи: динамично моделиране, пусков процес, двигателен момент, мощност, конусна инерционна трошачка, дебалансен вибратор, механична характеристика на асинхронен двигател

Introduction

Systems using unbalanced vibrators are not so well described in the terms of dynamical calculation. As it is well known the vibrator is rotating around its support shaft and the resistance over the shaft comes only from the friction because of orthogonal dynamical force and its speed. This is one of the main advantages of the vibrator, but it causes calculation problems.

Thereby the presented paper deals with the study of the starting process of the unbalanced vibrator within comparison between theoretical simulation model and experimental results.

As a representative of advanced crusher type the cone inertial crushers use a main driving system with unbalanced vibrator. The presented paper used the results and recordings from study of a cone inertial crusher type Mekhanobr KID-300 placed in laboratory of Department of Processing and Recycling of Mineral Resources in University of Mining and Geology "St. Ivan Rilski" with great acknowledgments to department head and staff.

The presented methodic follows the steps of installed machine power dynamical research in order to find the more economical way of materials crushing and effective power usage.

Dynamical modeling

Simulation study uses rotary three mass dynamical model with three degrees of freedom of the drive system of the machine (Savov and Nedialkov, 2014 (UMG pp. 11–14)). The drive system of the internal cone of the KID-300, shown on fig. 1, consists of an electric motor (1), V-belt transmission (2), an flexible rubber coupling (3), transmission constant velocity joined (cardan) shaft (4) and an adjustable unbalance vibrator (5). To simplify the theoretical study of the rotation model there were used the following idealizations:

– the system performs only a rotational movement around an axis (rotation about the vertical axis *z*);

– the kinetic energy of the system have only a rotary components;

– it is considered only linear resistance in the left part of differential equations (eq. 1), presented by Relay dissipative function;

– some elements are united with assumption that they are rotating with the same angular speed in entire bodies presented a summary of their inertia, namely:

   1. the rotor of the motor and the driven pulley;

   2. the rotating parts of the supporting block with the transmission shaft and unbalanced vibrator;

– resistances of friction in rolling and sliding support bearings are presented with a common resistance torque M_{l1};

– vibrator cylindrical roller bearing is presented with the speed dependent resistance torque M_{l2}, according to the "Jersey-Striebeck" diagram, witch parameters are presented in previous works (Savov and Nedialkov, 2014 (BJED); Nedyalkov, 2014).

Based on the upper described assumptions and idealizations, the drive system shown in figure 1 can be considered completely determined with parameters as it shown bellow.
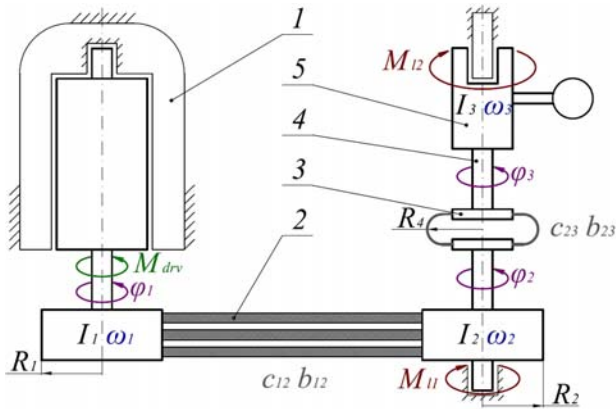

Fig. 1. Rotary three mass dynamical model

The model shown on fig. 1 is indexed with the following symbols:

I_1 – mass inertia moment of body №1 (induction motor rotor with driver pulley);

I_2 – mass inertia moment of body №2 (driven pulley);

I_3 – mass inertia moment of body №3 (support block, constant velocity joint (cardan) shaft and unbalanced vibrator);

ω_1, ω_2, ω_3 – bodies angular speed;

φ_1, φ_2, φ_3 – bodies rotation;

c_{12} – stiffness coefficient of element connection between body №1 and body №2 (belt stiffness);

c_{23} – stiffness coefficient of element connection between body №2 and body №3 (flexible coupling stiffness);

b_{12} – dissipative element connection between body №1 и №2, modeling belt dissipative properties;

b_{23} – dissipative element connection between body №2 and body №3, modeling flexible coupling dissipative properties;

M_{drv} – driver torque;

M_1 – summary resistance torque of support bearings;

M_2 – resistance torque in cylindrical sleeve bearing;

R_1 – driver pulley radius;

R_2 – driven pulley radius;

R_4 – flexible coupling radius;

$k_R = R_2/R_1$ (i_{rp}) – belt pulleys proportional coefficient (belt ratio).

The dynamic rotation multi mass model was built based on the second order Lagrange differential equations (Nedyalkov, 2009; Savov and Nedialkov, 2014 (UMG pp. 11–14); Savov, 2014). The system of differential equations describing the motion of a rotating three mass model (Savov and Nedialkov, 2014 (UMG pp. 11–14); Mitrev, 2004) is:

$$
\begin{vmatrix}
I_1.\ddot{\varphi}_1 + c_{12}.R_1^2.(\varphi_1 - k_R.\varphi_2) + b_{12}.R_1^2.(\dot{\varphi}_1 - k_R.\dot{\varphi}_2) = M_{drv} \\
I_2.\ddot{\varphi}_2 - k_R.c_{12}.R_1^2.(\varphi_1 - k_R.\varphi_2) + c_{23}.R_4^2.(\varphi_2 - \varphi_3) - \\
\quad - k_R.b_{12}.R_1^2.(\dot{\varphi}_1 - k_R.\dot{\varphi}_2) + b_{23}.R_4^2.(\dot{\varphi}_2 - \dot{\varphi}_3) = -M_{l1} \\
I_3.\ddot{\varphi}_3 - c_{23}.R_4^2.(\varphi_2 - \varphi_3) - b_{23}.R_4^2.(\dot{\varphi}_2 - \dot{\varphi}_3) = -M_{l2}
\end{vmatrix} \quad (1)
$$

The differential equations shown in matrices are:

$$
\begin{bmatrix} I_1 & 0 & 0 \\ 0 & I_2 & 0 \\ 0 & 0 & I_3 \end{bmatrix} * \begin{bmatrix} \ddot{\varphi}_1 \\ \ddot{\varphi}_2 \\ \ddot{\varphi}_3 \end{bmatrix} +
$$

$$
+ \begin{bmatrix} b_{12}.R_1^2 & -k_R.b_{12}.R_1^2 & 0 \\ -k_R.b_{12}.R_1^2 & k_R^2.b_{12}.R_1^2 + b_{23}.R_4^2 & -b_{23}.R_4^2 \\ 0 & -b_{23}.R_4^2 & b_{23}.R_4^2 \end{bmatrix} * \begin{bmatrix} \dot{\varphi}_1 \\ \dot{\varphi}_2 \\ \dot{\varphi}_3 \end{bmatrix} +
$$

$$
+ \begin{bmatrix} c_{12}.R_1^2 & -k_R.c_{12}.R_1^2 & 0 \\ -k_R.c_{12}.R_1^2 & k_R^2.c_{12}.R_1^2 + c_{23}.R_4^2 & -c_{23}.R_4^2 \\ 0 & -c_{23}.R_4^2 & +c_{23}.R_4^2 \end{bmatrix} * \begin{bmatrix} \varphi_1 \\ \varphi_2 \\ \varphi_3 \end{bmatrix} = \quad (2)
$$

$$
= \begin{bmatrix} M_{drv} \\ -M_{l1} \\ -M_{l2} \end{bmatrix}
$$

Geometry, inertial and dissipative model parameters, and the parameters of the elastic elements are defined according to Savov (2014) and are shown in table 1 together with their dimensions.

Table 1. *Dynamical model parameters*

Model Inertia parameters		
Parameter	Value	Unit
I_1	0,2411	kg.m²
I_2	0,0781	kg.m²
I_3	0,4109	kg.m²
Dissipation model parameters		
Parameter	Value	Unit
b_{12}	150,2	N.s/m
b_{23}	523,06	N.s/m
Stiffness model parameters		
Parameter	Value	Unit
c_{12}	277357,8	N/m
c_{23}	426137,4	N/m
Geometry model parameters		
Parameter	Value	Unit
R_1	0,098	m
R_4	0,08	m
k_R (i_{rp})	1,47	–

Driver and resistance torques used in dynamical model

Constant driver torque and constant resistance torque

Methodic of dynamic model synthesis, parameters identification and research results were presented (Savov and Nedyalkov, 2014 (UMG pp. 11–14)), in which the differential equations of motion were studied with linearized right side. In this dynamic simulation model M_{drv} was noted as constant torque determined according to Savov (2014), respectively M_p^{max} = 159,375 N.m

The value of the total resistance torque of sliding and rolling bearings in the vibrator drive system with some qualifications may be considered for the value of M_{pl} = 15,02 Nm in the cylindrical roller bearing (Savov and Nedialkov, 2014 (BJED)) increased by 20% and obtained M_{l2} = 18,02 Nm, M_{l1} = 0 Nm.

Driver characteristics and non linear resistance in the bearings

Crusher driver system use an induction motor with "squirrel" cage rotor and its catalogue parameters are presented in table 2.

Table 2. *Driver catalogue parameters*

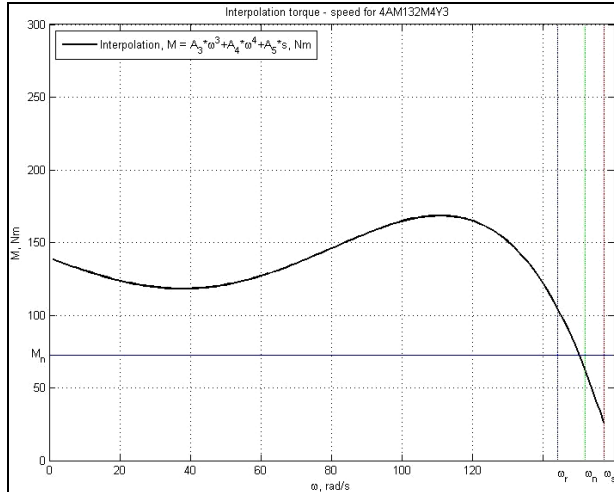| type	n_n	P	I_n	s_n	η	$Cos\varphi$
	min^{-1}	kW	A	%	%	
4AM 132 M4 У3	1450	11	22	2,8	87,5	0,86
	k_{max}	s_{max}	k_p	k_{min}	k_{lp}	
		%				
	2,2	19,5	2	1,6	7,5	

Fig. 2. Speed – torque characteristics interpolation

Asynchronous motors are with a non-linear mechanical characteristic depending on the slip between the angular speed of the stator field and the angular speed of the rotor. The theoretical construction of this dependence (Krawczyk et al., 1982) requires the synthesis of an electromechanical model including replacement circuit diagram of the motor and slip. For the purpose of this paper is used simplification which avoids compiling electromechanical model and a mechanical characteristic of the engine is interpolated according to fig. 2 with the following polynomial:

$$M_{drv} = A_3.\omega_1^3 + A_4.\omega_1^4 + A_5.s, \quad N.m \quad (3)$$

where:
A_i – interpolation polynomial coefficients;
ω_1, rad/s – driver angular speed;

$$s = \frac{\omega_s - \omega_1}{\omega_s}.100, \quad \% \ – \ \text{an induction motor slip, where:}$$

$$\omega_s = \frac{\pi.n_s}{30} = \frac{\pi.1500}{30} = 157,08 \quad rad/s \ – \ \text{is a driver}$$
synchronous angular speed.

The polynomial interpolation (eq. 3), was obtained with regression coefficient R^2 = 98,96% and is selected so that it follows the induction motor catalogue data and theoretical characteristic (Krawczyk et al., 1982). There are also studied similar polynomials of fourth degree and hyperbolic relationships, but they yield further amendments to the slope of the graph, shifting peaks, etc. Noted polynomial has a relative difference of up to 4% of the characteristic points of the engine to the range of the nominal slip. In order to minimize those differences propelling point is interpolated with the following functional dependence:

$$\left| \begin{array}{l} M_{drv} = A_3.\omega_1^3 + A_4.\omega_1^4 + A_5.s, \ at \ 0 \le \omega_1 \le \omega_r \ \& \ 100 \le s \le s_r \\ M_{drv} = 104,27 \ N.m, \ at \ \omega_r < \omega_1 < \omega_n \ \& \ 100 \le s \le s_r \end{array} \right. \quad (4)$$

where:

$$\omega_r = \frac{\pi.n_{uv}}{30.i_{rp}} = \frac{\pi.2023}{30.1,47} = 144,11 \quad rad/s \ – \ \text{is a driver}$$
working angular speed counted with optical tachometer;

$$\omega_n = \frac{\pi.n_n}{30} = \frac{\pi.1450}{30} = 151,84 \quad rad/s \ – \ \text{is a driver}$$
nominal angular speed;

$$s_r = \frac{\omega_s - \omega_r}{\omega_s}.100 = \frac{157,08 - 144,11}{157,08}.100 = 8,257 \quad \%,$$

where s_r is a slip at working angular speed.

Resistance torque of sliding bearing is interpolated as follows:

$$M_{l2} = B_0 + B_1.\omega_3 + B_2.\omega_3^2, \quad N.m \quad (5)$$

Resistance torque of sliding bearing is a complex dependent as a function of the angular velocity of the unbalance vibrator $\omega_3 \equiv \omega_{uv}$, the viscosity of the oil and other operating parameters of the node (Savov and Nedyalkov, 2014 (BJED)). Resistance torque is interpolated with a second order polynomial function with sufficient accuracy (R^2=99,92%) where B_i are the coefficients of the polynomial interpolation. The value of the total resistance of the rolling bearings in the drive system M_{l1} is accepted 20% of the value of the torque resistance in the cylindrical roller bearing.

Simulation results

The presented rotary three mass model was performed with a simulation study of starting process of unbalance vibrator in a programming environment with MatLab. The settings of the

13

machine used in simulations are taken from experimental conditions and set up of the machine as follows:

– temperature of the working fluid t = 30,5°C (measured experimentally);

– mass static moment of unbalance vibrator S_{uv} = 1,289 kg.m (18th degree of unbalance vibrator);

– speed of the unbalance vibrator n_{uv} = 2023 rpm (f = 33,72 Hz - measured experimentally).

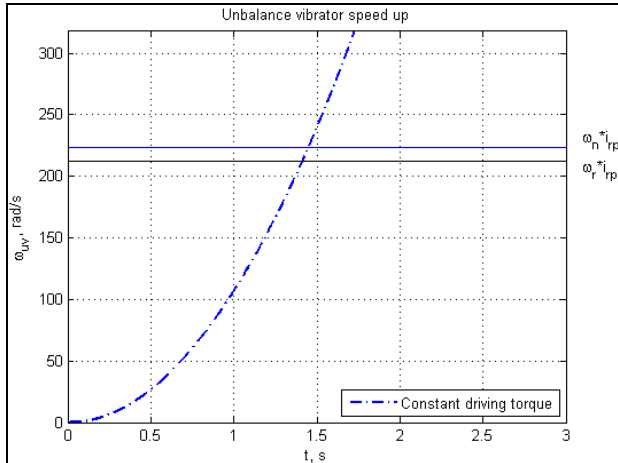**Simulation results with constant driving and resistance torques**

Fig. 3. Starting process with constant driving and resistance torques

Results of the survey with constant driving and resistance torques in appropriate settings of the machine are presented in fig. 3. At fig. 3 is recognized that the time required for acceleration of the unbalance vibrator (to work angular velocity ω_{uv} = 211,85 rad/s) is obtained t_{p1} = 1,459 s.

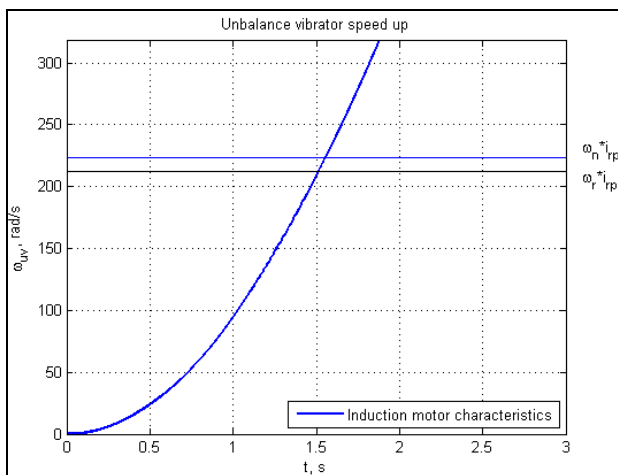**Simulation results with non-linear driving and resistance torques**

Fig. 4. Starting process with non-linear driving and resistance torques

Starting survey is with particular data – appropriate settings of the machine are shown on fig. 4. From the intersection of the characteristic presenting mode acceleration of unbalance vibrator and characteristics corresponding to the rated speed of the unbalance vibrator (experimentally determined) can be read the time required for acceleration of the unbalance vibrator from the placing of the drive motor to reach nominal angular velocity of unbalance vibrator.

Fig.4 shows that the time required for acceleration of the unbalance vibrator (to work angular velocity ω_{uv} = 211,85 rad/s) is obtained to t_{p2} = 1,521 s.

Experimental research of starting process

Vibrogage measurement system (Nedialkov, 2009) used here contains uniaxial piezo-electric transducers KD35, preamps (Charge Amp) and gain stage of instrumental amplifiers Inst Amp as a classical (Craig, 1989; De Silva, 2000) piezo measurement system. The schematically layout of the sensors on the KID-300 is presented on fig. 5.
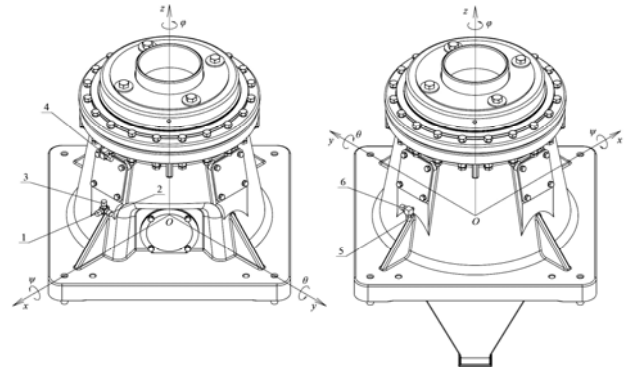

Fig. 5. Accelerometer gage schema over the KID 300 housing

Measurement system amplifier is connected to the computer system using National Instruments NI USB 6210 analog-to-digital converter (ADC) with USB interface. The flow of data after ADC is processed in digital form by recording the data in a file was made with computer application DASYLab® (Savov and Nedyalkov, 2014 (UMG pp. 15–18)).

Experimental results

The experimental study was done under the same conditions (machine settings) as well as in the simulation study. Computer recorded signal needs a process to extract the necessary information. Using the software OriginPro fig. 6 presents one of the recordings processed, noted recording of signal received from sensor №3 (fig. 5).
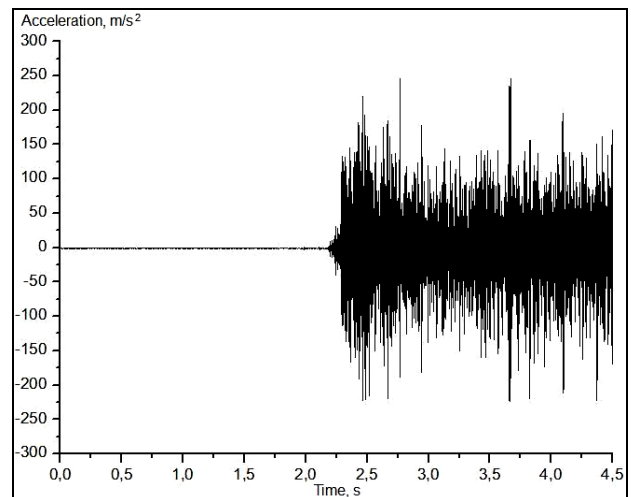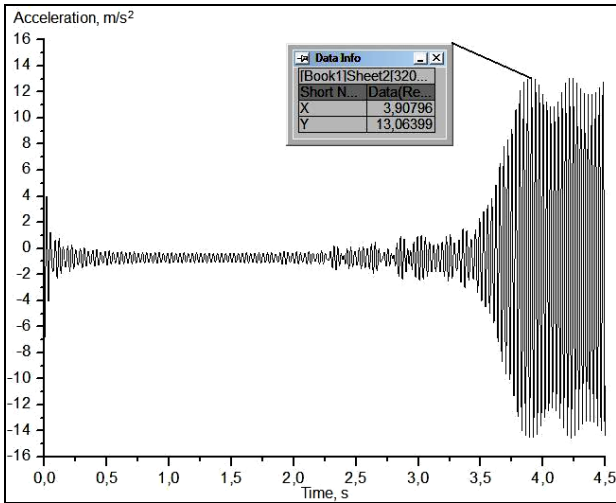

Fig. 6. Experimental records from sensor №3

The experimental record is filtered using a Band Pass FFT filter for frequency range 30÷40Hz. Figure 7 presents the result of the filtered recording signal (Fig. 6) of the sensor №3. Figure 7 shows that the unbalanced vibrator is at normal operating angular velocity of ω_{uv}=211,85 rad/s at 3,908 s.

Фиг. 7. Band pass (30÷40 Hz) filtered sensor №3 signal

From records deposition (fig. 8) of the signals from the sensor №3 and the filtered signal (for the frequency range 30÷40 Hz) can be determined the beginning of the starting process of the driving motor. According to fig. 8, the drive motor is switched on 2,191 s.
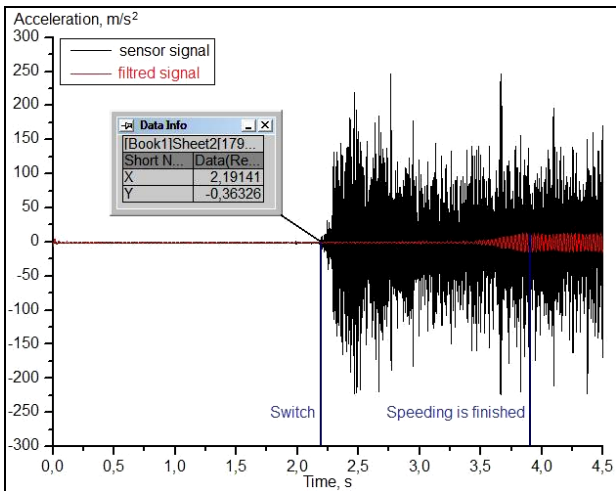

Fig. 8. Experimental records from sensor №3 and the same filtered signal – band pass (30÷40 Hz).

The difference in the times obtained from fig. 7 and fig. 8 represents the duration of the starting process of the machine (unbalance vibrator). Time for which the unbalance vibrator is at normal operating angular velocity of ω_{uv}=211,85 rad/s at the time of inclusion of the drive motor is t_{p3}=1,717 s.

Conclusions

The results obtained on the duration of the starting process of the drive system of the crusher type of KID rotary dynamic simulation model that takes into account the non-linear nature of the engine torque of the drive motor and modulus in the cylindrical journal bearing with higher accuracy compared with the simulation model in engine and modulus are constant respectively:

– the relative difference in results obtained from simulation study of the process of acceleration with constant driving and resistance torques compared to results of experimental study of unbalance vibrator speed up is -15,03%;

– the relative difference in results obtained from simulation study of the process of acceleration with non-linear driving and resistance torques compared to results of experimental study of unbalance vibrator speed up differs a few sub results shown in table 3 and fig. 9 explained as follows:

1. speeding up to a working speed ω_r = 144,11 rad/s wich results in M_r = 104,27Nm, and time 1,521s with relative difference to experimental result - 11,42%;

2. speeding up to a working speed ω_r = 147,12 rad/s wich results in M_r = 89,54 Nm, and time 1,590 s with relative difference to experimental result - 7,4 %;

3. speeding up to a nominal working speed ω_r = 151,84 rad/s wich results in nominal driver torque M_r = 72,45 Nm, and time 1,604 s with relative difference to experimental result - 6,58 %;

The convergence in simulation results compared to the experimental is very good and hit nearby the normal engineering error. Thus the simulation models are accepted with very good convergence to the experimental set up.

As a future work it is expected to install the more precise tachometers on both shafts – driver and vibrator shafts, to ensure exact recording of speed up process neglecting the shaft speed differences and speed up exact counting.
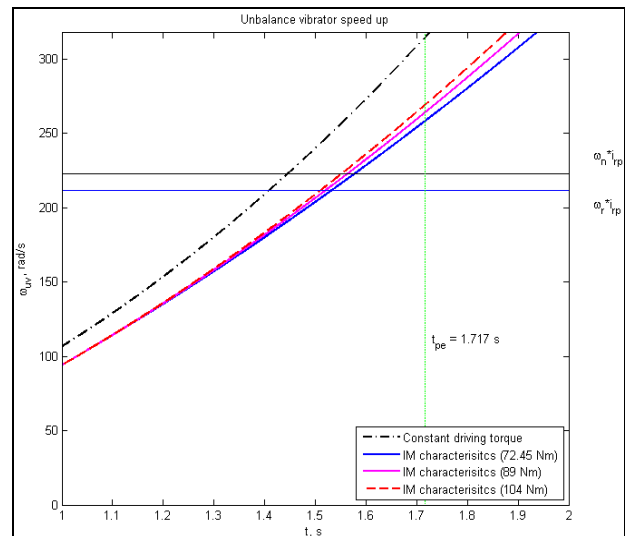

Fig. 9. Comparison between simulation and experimental results

Table 3. *Comparison between simulation and experimental results*

	Exp.	Simulation			Simulation
	M_n	**M_n**			const. **M**
M_r, N.m	72,45	72,45	89,54	104,27	72,45
M_{start}, N.m	130,41	nonlinear M (torques)			159,39
ω_r, rad/s	151,84	151,84	147,12	144,12	151,84
s_r, %	3,33	3,33	6,34	8,25	3,33
t_p, S	1,717	1,604	1,59	1,521	1,459
ε, %	-	6,58	7,40	11,42	15,03

15

References

Craig J. *Introduction to robotics, mechanics and control.* Addison-Wesley Longman, Boston, Second edition, USA, 1989.

De Silva C. *Vibration: fundamentals and practice.* CRC Press Boca Raton, London New York Washington, USA, 2000.

Ganiev R., V. Kononenko. *Kolebaniya tverduih tel.* Moscow, Nauka, 1976. (in Russian)

Krawczyk A., M. Schlaff, et al. *Spravochnik asinhronnuie dvigateli serii 4A.* Energoizdat, Moscow, 1982. (in Russian)

Mitrev R. *Mechano-mathematical modeling of process and machine for vibroseparation.* Avtoreferat, TU-Sofia, 2004. (in Bulgarian)

Nedyalkov P. *Dinamical modeling and research of working process and parameters of vertical vibro-impulse comminution mill.* Avtoreferat, TU-Sofia, 2009. (in Bulgarian)

Nedyalkov P. FEM modeling and characteristics research of cylindrical journal bearing for cone inertial crusher /KID-300/. *RECENT*, Vol. 15, № 2(42), July 2014, Brashov, Romania, pp. 112–116, ISSN 1582-0246 & ISSN 2065-4529.

Savov. S., P. Nedyalkov. Dynamical modeling of driver system of cone inertial crusher type KID-300. *Annual of the University of Mining and Geology "St. Ivan Rilski"*, Vol. 57, Part III, Sofia, 2014, pp. 11–14. (in Bulgarian)

Savov S., P. Nedyalkov. Experimental measurement methodic for vibration parameters of cone inertial crusher type KID-300. *Annual of the University of Mining and Geology "St. Ivan Rilski"*, Vol. 57, Part III, Sofia, 2014, pp. 15–18. (in Bulgarian)

Savov S., P. Nedyalkov. Research over a cylindrical journal bearing of one cone inertial crusher (KID-300). *Bulgarian Journal for Engineering Design*, Issue 21, January 2014, pp. 17–22, ISSN 1313-7530. (in Bulgarian)

Savov S. *Research of mechanical and technological parameters of cone inertial crushers type KID.* Dissertation, University of Mining and Geology "St. Ivan Rilski" – Sofia, 2014. (in Bulgarian)